

# INFLUENCE OF SURFACE TOPOGRAFY ON ZIG-ZAG DEFECTS IN FERROELECTRIC LIQUID CRYSTAL DISPLAYS

J. Pirš, R. Petkovšek, S. Pirš, S. Kralj and S. Žumer  
J. Stefan Institute, Ljubljana, Slovenia

**Keywords:** LC, Liquid Crystals, Liquid Crystal Cells, SmC liquid crystals, Smectic C liquid crystals, chevron structures, zig-zag defects, LANDAU-GINZBURG theory, nematic director field, smectic complex order parameters, threshold conditions, cost estimation, practical results, theoretical results

**Abstract:** The influence of surface conditions on chevron structures and zig-zag defects in a SmC liquid crystal cell is studied both experimentally and theoretically. In order to gain insight into basic properties of the system the Landau-Ginzburg type theory is used in terms of the nematic director field and the smectic complex order parameter. On a simple model system transitions in the C1 and C2 chevron structures are studied as functions of the surface pretilt angle  $\theta_t$ . The threshold conditions are calculated. The width of the straight element of the domain wall (running parallel to smectic layers) and the costs for its formation are estimated. In the experimental part of the work the effect of the confining substrate with controlled variation of the surface slope on the formation of zig-zag defects is analysed. Observed results are in line with theoretical expectations.

Pacs numbers: 61.30.Jf, 64.70.Md

## Vpliv površinskih pogojev na strukturo zig-zag defektov v feroelektričnih LCD prikazalnikih

**Ključne besede:** LC kristali tekoči, celice kristalov tekočih, SmC kristali tekoči C smektični, chevron strukture, cik-cak hibe, LANDAU-GINZBURG teorija, polje nematično direktorsko, parametri smektični reda kompleksnega, pogoji pragovni, ocena stroškov, rezultati praktični, rezultati teoretični

**Povzetek:** Preučevali smo vpliv površinskih pogojev na strukturo ševronov in zig-zag defektov v SmC tekočem kristalu, omejenem v planparalelni celici. Kvalitativno obnašanje sistema smo ocenili izhajajoč iz Landau-Ginzburgove proste energije, izražene z nematičnim direktorskim poljem in smektičnim kompleksnim ureditvenim parametrom. Na poenostavljenem modelu smo preučevali prehode med ševronskima strukturama C1 in C2 v odvisnosti od nagiba molekul ob površini celice. Izračunali smo kritični pogoj prehoda. Ocenili smo širino in potrebno energijo za tvorbo domenske stene med področjima različne orientacije ševrona. V eksperimentalnem delu smo preučevali vpliv površine s kontrolirano variacijo površinskega nagiba na nastanek zig-zag defektov. Opaženi rezultati se kvalitativno ujemajo s teoretičnimi napovedmi.

### I. INTRODUCTION

Basic ingredients of various electrooptic devices are smectic C (SmC) liquid crystals (LC) confined to plan-parallel cells where smectic layers run along cells. In most cases chiral SmC LCs are used (SmC\*) because of their ferroelectric properties. These layered configurations are enabled by planar anchoring /1/ or anchoring with a small pretilt. It often happens that the confining surfaces impose a periodicity  $q_s$  which in general differs from the intrinsic bulk SmC periodicity  $/2,3/q$ . In most cases the origin of the surface periodicity is a thin single molecular LC layer relatively strongly bounded to the surface (i.e. the mobility of molecules in this layer is strongly restricted in comparison to the bulk). The surface periodicity  $q_s$  is believed to be fingerprinted and frozen in on entering the smectic phase /2/. In the particular case of  $q=q_s$  the bookshelf structure (see Fig. 1a) is established. While in general  $q \neq q_s$  yielding an uniformly distributed strain on the bookshelf structure. If  $q_s < q$  and if a threshold condition is fulfilled /3,4,5/ the confined smectic LC can substantially reduce the strain by converting into a chevron one or in some cases into a tilted structure schematically shown in Figs. 1b,c. In both structures layers are tilted with respect to the surface enabling the smectic layer spacing to match the one preferred by the surface and smectic

elastic constants in most of the cell. The homogeneously tilted structure has lower free energy. But its realisation requires that layers slip at the surface. In practice this process is exceedingly slow so that the chevron structure with a kink in the middle of the cell is usually realised instead /6,7/. In the case with kink the elastic deformations are constrained to the surface and the chevron tip. Details are given in ref. /4/.

For ideal planparallel geometry and planar anchoring the chevron tip can orient in either of the two directions perpendicular to layers as both directions are energetically equivalent. This degeneracy is broken if layer thickness spatially vary or a finite surface anchoring pretilt is introduced. The chevron configurations in which layers are tilted in the tilt direction are conventionally referred to as the C1 structure /8/. The C2 structure describes the opposite case as shown in Fig. 1d. Experimental results /8/ suggest that the existence and stability of these structures in the SmC phase strongly depend on the relative value of the surface pretilt angle  $\theta_t$  with respect to the bulk tilt angle  $\theta_c$  between the layer normal and the average orientation of long axis of molecules ( $\theta_c$  is the order parameter of the SmA-SmC phase transition). A kind of threshold behaviour is observed exhibiting strong hysteresis behaviour /8/. For a large enough surface pretilt only the C1 structure can

exist. For low pretilts both the C1 and C2 structure exist but only the C2 structure seems to be stable.

In most cases domains with either C1 or C2 structure forms. The domain walls, where the chevron tip orientation reverts (see Fig.1e), are conventionally named zig-zag defects /2/. There exist various qualitatively different forms of these defects. The most simple structure is realised for the "head to head" chevron collision in which the domain wall runs parallel to smectic layers and has thus straight linear appearance. In this scenario significant spatial deviations from a monodomain structures are only along the layers' normals. Reorientation of the kink is mediated by a quasi bookshelf structure /9/. Across the wall the smectic interlayer separation does not show noticeable variation. The wall width is estimated to be roughly of the cell width /2,9/L. This wall structure is stable for the  $\gg \parallel \ll$  like transition (symbol  $\parallel$  describes the wall and  $\gg$  gives the direction of the kink far from the wall). In  $\ll \parallel \gg$  transition the wall has in almost all cases strong zig-zag appearance according to which it is also named.

These most commonly qualitatively different scenarios of the wall organisation for the  $\gg \parallel \ll$  and  $\ll \parallel \gg$  transition indicate that they are considerably different from the energetical point of view. In the "head to head" wall scenario the layers experience strain concentration at the center of the wall which gradually decreases on going away from the center. In the case of  $\ll \parallel \gg$  transition it seems that the strain is large enough to initiate the rearrangement of the surface ordering /2,7/. This process is believed to be extremely slow and is

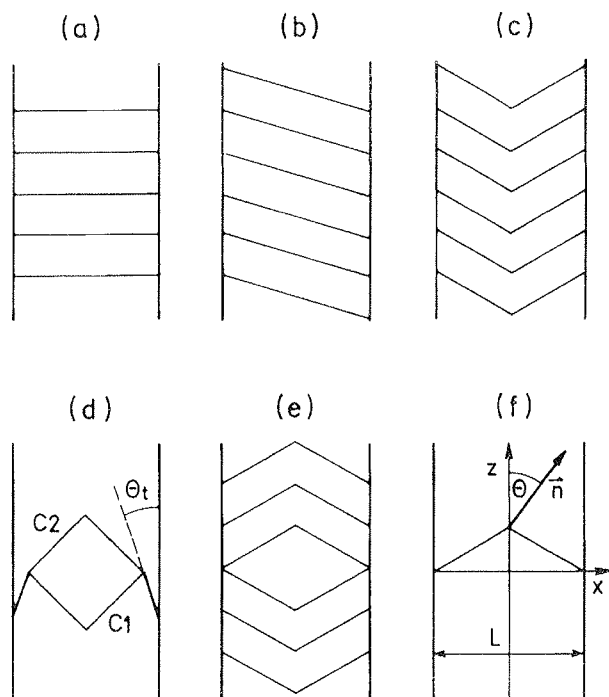


Fig.1 Schematic presentation of the (a) bookshelf, (b) tilted, (c) chevron, (d) C1, C2 and (e) zig-zag layer structure. In (d) the surface strongly enforces a finite pretilt  $\theta_t$ . The co-ordinate system used in calculations is shown in (f).

realised if the system can not relax the imposed dilation in a different way /4,7/. The surface rearrangements partially relax the strain imposed on the layers enabling narrower domain walls whose direction makes finite angle with respect to the chevron tip orientation /2/. The course of such a wall is zig-zag in appearance and is believed to be controlled by various disturbances in the system (thus the zig-zag pattern is not an inherent property of the LC).

The presence of zig-zag defects is in most applications not desired because its pattern is hard to be controlled and reduces the optical properties of cells /8/. In order to avoid them it is essentially to understand reasons for their appearance. They can be among others induced by surface irregularities /2,8/ (i.e. spatial variation of the surface profile, surface anchoring condition...). The aim of this paper is to develop a theoretical explanation of our recent experiments /10/ on the influence of the controlled surface slope or pretilt on the formation of zig-zag defects.

The paper is organised in the following way. In Sec. 2 the experimental part of the work is presented. In Sec. 3 the model is presented providing qualitative explanation of the experimental results. Stability of the C1 and C2 structure and the free energy costs to form domain walls is studied. The experimental results are discussed in the Sec. 4 and conclusions are summarised in the last section.

## II. EXPERIMENTAL SET UP

This paper as well as other publications /10,11,12/ present experimental evidence, that the surface topography plays a very important role in the surface stabilised SmC\* thin film liquid crystalline layers. Studies of the "chevron defect" density show, that even very small orienting surface defects can cause the instability of the chevron structure as long as the slope of these defects is high enough. Fig. 2a shows an AFM photograph of a relatively flat rubbed nylon (DuPont Elvamide 6) surface deposited on the flat glass surface by dip coating, polymerised at 120°C and slowly cooled to the room temperature (conventional method). Such a surface treatment is often used to enforce homogeneous anchoring of LC molecules with a small pretilt. It is evident that real surfaces used in LC cells are far from being "flat", what is conventionally assumed in theoretical models used to study LC structures.

The aim of this study is to exploit the influence of sloped regions introduced by surface irregularities on the appearance of zig-zag defects. In order to do this we first made a flat reference surface using the "heat quenching method" developed /10,12/ by Pirš et al. The gist of this method is (i) adequate doping of the nylon used for the cell coating and (ii) heating the polymer layer approximately 10°C above its glass transition temperature ( $\approx 160^\circ\text{C}$ ) and submitting it to a thermal shock, by fast cooling to the room temperature. This procedure prevents the crystallisation process within the polymer, which is the main reason for surface roughness as seen on the Fig. 2a. Consequently extremely flat amorphous

nylon surface is formed. This is evidently shown in Figs. 2 where the nylon treated surface formed by (a) conventional and (b) "heat quenching" method are compared.

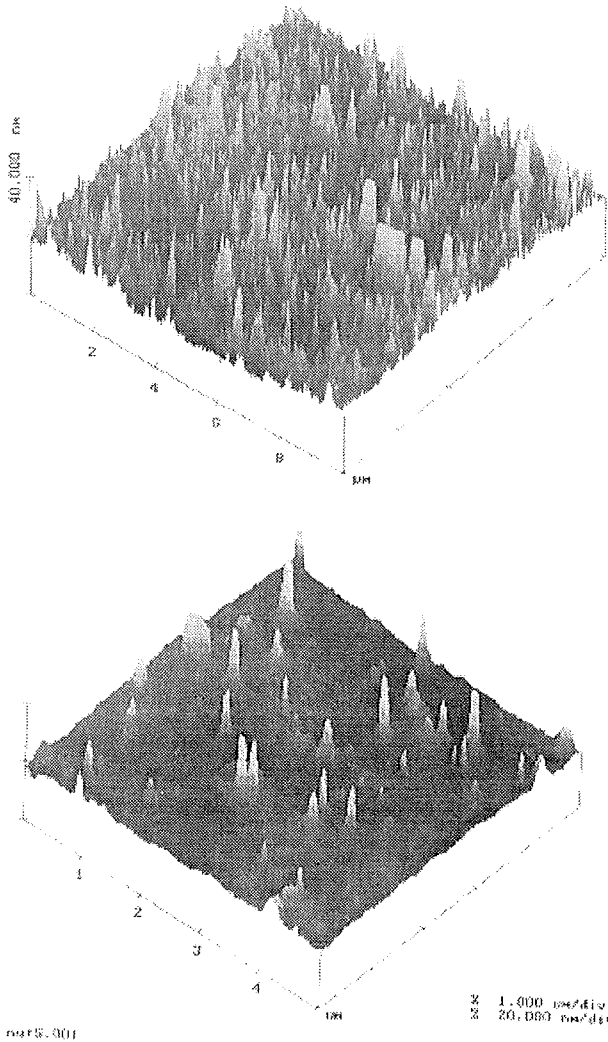


Fig. 2 The AFM images (tapping mode) of a nylon treated surface formed by (a) conventional, (b) "heat quenching" method. In (a) the surface exhibits strong spatial departures from the "ideal planarity" because of the crystalline domains formed within the nylon surface coating. In (b) the crystallisation process is on the average strongly suppressed yielding extremely flat surface.

The real SSFLC display orienting surface as presented on Figs.2 in not very convenient for comparison with theoretical models and a more defined and regular surface is needed for better understanding of the surface topography problems. In order to form a controlled surface slope a long straight Chromium stripe was deposited on the flat reference surface. Both edges of the stripe were polished, yielding slopes with relatively well defined inclination and then covered with doped nylon and heat quenched as described above. A typical AFM photograph of a resulting slope is shown in Fig. 3.

The resulting local cell geometry is schematically shown in Fig. 4a. The height  $\Delta H_x$  and the length  $\Delta H_z$  of each sloped area is  $0.1 \mu\text{m}$  and  $0.2 \mu\text{m}$ , respectively. The corresponding slope is  $\theta_s = \text{Arctan}(\Delta H_x / \Delta H_z) \approx 27^\circ$ . The cell width  $L$  is  $1.5 \mu\text{m}$  and the separation  $H_s$  between the sloped areas is  $50 \mu\text{m}$ , thus of finite width with respect to  $L$ . The cell surface was nylon treated and rubbed, enforcing a finite pretilt  $\theta_t \approx 3^\circ$ .

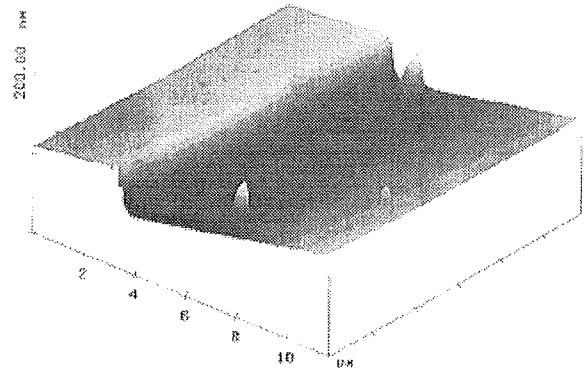


Fig. 3 The AFM photograph of the polished Chromium step. The inclination of the sloped region is relatively well defined.

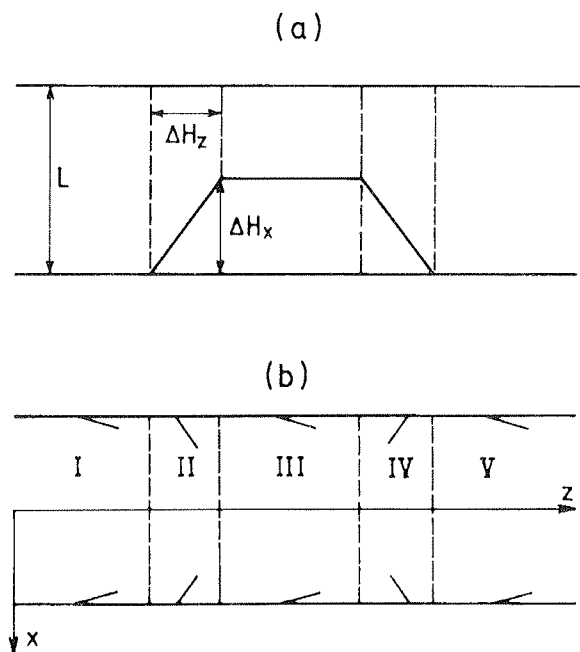


Fig. 4 a) Schematic presentation of the experimental set-up. (b) The spatial variation of the surface slope is within the model imitated by spatially dependent pretilt  $\theta_t$ . The sample is divided into regions (i), (ii), (iii), (iv) and (v). The pretilt  $\theta_t = \theta_p \approx 3^\circ$  in regions (i), (iii) and (v) is achieved by a nylon surface treatment. The left slope of the region (ii) is simulated by the surface tilt  $\theta_l = \theta_s + \theta_p \approx 30^\circ$  and the right one of the region (iv) by  $\theta_r = -\theta_s + \theta_p \approx -23^\circ$ .

The surface was buffed along the stripe (i), as well perpendicular to this direction (ii). Only in the case (ii) the zig-zag defects were formed at sloped stripes. Approximately 10% of the length along each polished step (y-direction) initiated closed zig-zag loops. The reminding region exhibited a monodomain chevron orientation. An optical polarisation photograph under crossed polarisers of a typical region exhibiting zig-zag lines is shown in Fig. 5 (Note that the poor contrast of the photo is due to strong differences between the reflectivity of the Cr step and the rest of the surface). The photograph reveals that zig-zag lines are localised at the sloped stripes proving their responsibility for defect formation. The zig-zag patterns at the first and second slope are qualitatively different and so is also the region (relative to the stripe position) where they appear. The zig-zag lines do not have longer straight segments perpendicular to the tilt direction characteristic for the head to head chevron collision /2/. The width of lines is relatively narrow with respect to L.

In order to qualitatively understand the observed pattern we use a phenomenological theory to study influence of the pretilt on the chevron structure.

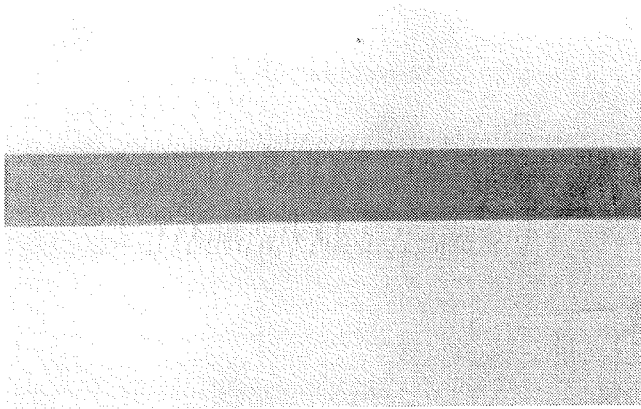


Fig.5 A photograph obtained via optical polarisation microscope with crossed polarisers showing zig-zag defects that originate mostly at the two sloped regions.

### III. FREE ENERGY

To calculate the chevron structure we use Landau-Ginzburg type free energy /1,5/. The LC structure is described in terms of the uniaxial nematic director field  $\mathbf{n}$  and the smectic complex order parameter  $\Psi = \eta e^{i\Phi}$ . The nematic orientational order parameter and smectic translational order parameter  $\eta$  are assumed to be spatially homogeneous while the phase factor  $\Phi$  describes the position of smectic layers. The corresponding relevant part of free energy is expressed as /5/

$$F = \int \left( \frac{K_{11}}{2} (\nabla \cdot \bar{\mathbf{n}})^2 + \frac{K_{22}}{2} (\bar{\mathbf{n}} \times \nabla \times \bar{\mathbf{n}})^2 + \frac{K_{33}}{2} (\bar{\mathbf{n}} \cdot \nabla \times \bar{\mathbf{n}})^2 + \right.$$

$$\left. + C_{||} |(\bar{\mathbf{n}} \cdot \nabla - q_0) \Psi|^2 + C_{\perp} |(\bar{\mathbf{n}} \times \nabla) \Psi|^2 + D |(\bar{\mathbf{n}} \times \nabla)^2 \Psi|^2 \right) d^3 \bar{\mathbf{r}}. \quad (1)$$

At the surface strong positional and orientational anchoring is assumed. The elastic properties of the enclosed LC are described by nematic ( $K_{11}$ ,  $K_{22}$ ,  $K_{33}$ ) and smectic ( $C_{||}$ ,  $C_{\perp}$ ,  $D$ ) elastic constants. In this study the so called /1/ surface or divergence nematic elastic constants ( $K_{24}$  and  $K_{13}$ ) do not play important role and are therefore discarded. Here  $q_0$  is the periodicity adopted in the SmA phase. Chirality which considerably affects the nematic director field /2/ is not of interest in this discussion since it does not significantly alter the layer structure.

Within the Landau-Ginzburg description /1,5/ the SmA-SmC transition is continuous and triggered by the smectic bend elastic constant  $C_{\perp}$ . The SmA phase is stabilised for  $C_{\perp} > 0$  and SmC for  $C_{\perp} < 0$ . The tilt  $\theta_c$  of molecules from the layer normal in the bulk SmC phase is  $\theta_c = \text{Arc tan}(-C_{\perp}/(2Dq_0^2))$  and the layer periodicity is  $q = q_0/\cos \theta_c$ .

Some qualitative predictions concerning the structure of the system can be inferred from the values of characteristic lengths entering the model. These are in addition to the cell thickness L the smectic penetration lengths

$$\lambda_{\perp} = \sqrt{K/(2\eta^2 C_{\perp} q_0^2)}, \quad \lambda_{||} = \sqrt{K/(2\eta^2 C_{||} q_0^2)}$$

and the length  $\lambda_c = \sqrt{D/(2C_{\perp})}$  characterising the thickness of the chevron tip /1,5/. The relative strength of the nematic and smectic contribution in Eq. (1) is of order  $(\lambda_{||}/L)^2$ . In the SmC phase  $\lambda_{||}$  is typically few molecular lengths. Consequently in supramicron cells the inequality  $\lambda_{||}/L < 1$  suggests that the LC structure is mainly governed by smectic elasticity.

### IV. MODEL CELL STRUCTURE

The geometry of the problem is depicted in Fig. 1f. The layers are running in the z direction. The cell plates are positioned at  $x = -L/2$  and  $x = L/2$  where L stands for the cell thickness. In the model we assume that LC molecules are restricted to the (x,z) plane. This approximation grossly simplifies the mathematics of the problem and conserves the qualitative features of the structure. In the model the surface rigidly imposes the periodicity  $q_s$  (strong positional anchoring limit) and the surface tilt  $\theta_t$  of surface LC molecules from the z-direction (strong orientational anchoring limit). The variational parameters  $\mathbf{n}$  and  $\Phi$  are parametrized as  $\mathbf{n} = (\sin\theta, 0, \cos\theta)$  and  $\Phi = q_s(z-u)$ , where u describes departures from the bookshelf layer structure.

First we study the existence and stability of C1 and C2 structures with respect to the relative value of  $\theta_t$  and  $\theta_c$ . For this purpose the variational parameters  $\theta$  and u are allowed to vary only in the x-direction. The threshold behaviour of the transformations between C1 and C2 structures is analysed.

We further estimate typical free energies to form a wall parallel to smectic layers that corresponds to the head to head collision of two chevrons. In this case the variational parameters are allowed to vary also in the z-direction. Since we are mainly interested in the layer structure we simplify calculations by performing them in a SmA phase. The smectic layer structure is dominantly determined by smectic elastic constants. Thus the effect of the "nematic" component (i.e. the so called  $\mathbf{c}$  director describing the projection of the director field in the smectic layer plane), which distinguishes between the SmA and SmC phase, is in this case of secondary importance. We enforce a chevron profile by imposing at the surface periodicity different from the one in the bulk.

Based on the results deduced from these model structures we qualitatively explain phenomena observed in our experiments. In the model we simulate the variation in the slope of the bounding surface in the experimental cell (Fig.4a) by a variation of the pretilt angle  $\theta_t$  assuming a perfectly flat surface (see Fig.4b). We anticipate that the spatial variation in the pretilt angle or surface topography have in most cases similar qualitative consequences on the chevron structure.

## V. CHEVRON STRUCTURE

### V.1 Influence of the pretilt $\theta_t$ on the chevron structure

We first study the influence of a homogeneous surface pretilt  $\theta_t$  on the chevron structure. Geometrical arguments [8] suggest that significant parameter relevant for the chevron structure is the ratio  $\chi = \theta_t / \theta_c$ . The influence of  $\chi$  on the chevron profile is depicted in Figs. 6a,b. The effect is demonstrated in relatively thin cells ( $L = 0.1 \mu\text{m}$ ) where  $L$  and  $\lambda_i (i = \perp, \parallel)$  are less apart and variations of both parameters are spreaded over a substantial part of the cell.

If  $\theta_t = 0$  then  $\theta(x) = 0$  everywhere and elastic distortions of smectic layers are constrained to the chevron tip. We refer to this structure as the "reference" structure. Both chevron orientations of the reference structure are equivalent. A finite pretilt introduces spatial variations of  $\theta$  across the cell. Results indicate that there exist critical (threshold) values of  $\chi$  (denoted by  $\chi_{C1}$  and  $\chi_{C2}$  corresponding to the C1 and C2 structure, respectively) separating qualitatively different regimes. For  $\chi > 0$  and  $\chi < \chi_{C1}, \chi_{C2}$  the departures from the reference chevron structure of the two profiles are constrained to a narrow region of a thickness  $\lambda_{\perp}$  at both cell surfaces. This region broadens with increasing  $\chi$  until a critical value  $\chi$  is reached ( $\chi_{C1}$  for C1 and  $\chi_{C2}$  for the C2 structure). At the critical value departures of  $\mathbf{n}$  from the reference structure spreads across the whole cell. This configurational transition is discontinuous.

Above the threshold (i.e.  $\chi > \chi_{C1}, \chi_{C2}$ ) both C1 and C2 structures convert into an identical structure, which we denote by C1\*, with the chevron tilt determined by the surface pretilt. Its main difference from the C1 structure is in a broader chevron tip and in a nematic director field which substantially departs from the z-direction across the whole cell. Despite this the smectic free energy density distribution is qualitatively similar below and above the transition although the jump in the total free energy can be in general substantial (see Fig. 7). The nematic splay distortion is shifted to the chevron tip and consequently its width is increased. Note that this effect on the chevron tip width is less evident in thicker cells. Thus for  $\chi > \chi_{C2}$  only C1\* or C1 structures are possible in agreement with experimental observations [8].

The threshold value  $\chi_{C1}$  and  $\chi_{C2}$  for both configurational transitions depend on elastic properties of the LC (thus also on  $\theta_c$ ) and the cell thickness. For  $L = 0.1 \mu\text{m}$  and conventional elastic constants we obtain critical value  $\chi_{C2} \approx 1.7 \pm 0.4$  while  $\chi_{C1}$  is typically 5% larger. For a choice of parameters given in the caption of Fig. 6 one

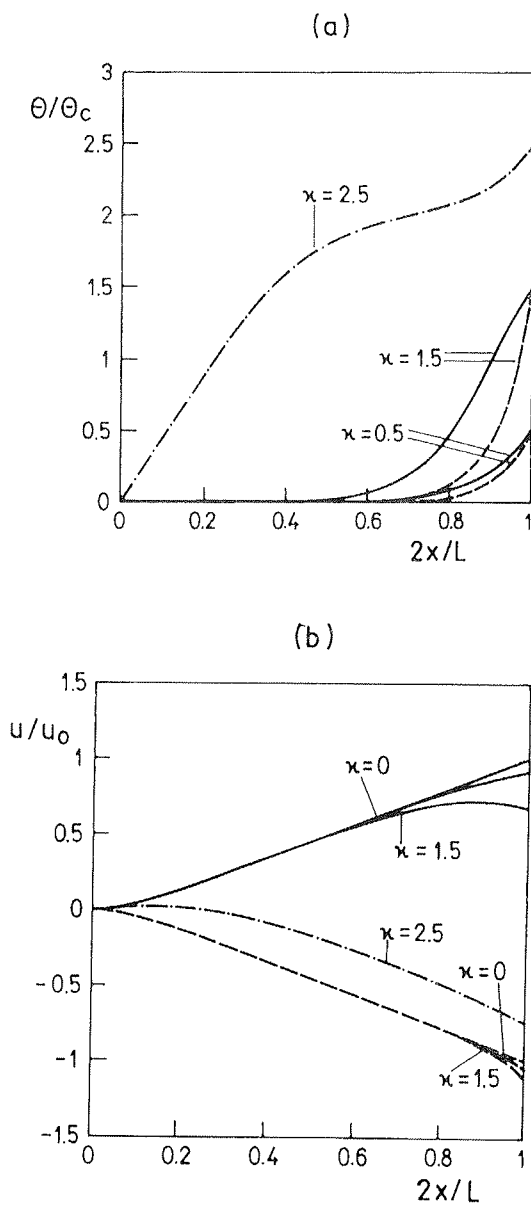


Fig. 6  $\theta(x)$  (a) and  $u(x)$  (b) dependence of the chevron structure for different values of  $\chi$ . In calculations we use  $L/\lambda_{\parallel} = 100$ ,  $L/\lambda_{\perp} = 10$ ,  $qL\lambda_c/\lambda_{\perp} = 100$ ,  $\lambda_c/\lambda_{\perp} = 1$ .  $u_0 = u(x=0)$  for  $\chi = 0$ .

finds  $\chi_{C2} \approx 1.95 \pm 0.05$  and  $\chi_{C1} \approx 2.05 \pm 0.05$ . These values are close to those obtained from simple geometrical considerations /8/.

The variation of the free energy (see Eq. (1)) of both structures with  $\chi$  is shown in Fig. 7. For any finite value of  $\chi$  the degeneracy between C1 and C2 structure is broken. Below critical value of  $\chi$  the C2 structure is stable in agreement with experimental results /8/.

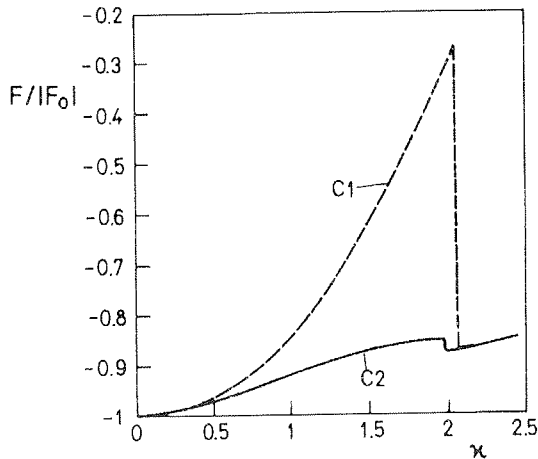


Fig. 7 Free energy of the chevron structures as function of  $\chi$ .  $F_0 = F(\chi=0)$ . Parameters are the same as in Fig. 6

### V.2 The domain wall

We next focus our interest to the domain wall of a head to head chevron collision. In an uniform cell this is not a stable structure but it can be stabilised by a particular variation of the surface induced pretilt. Within our model this wall can be realised only via an intermediate bookshelf-like region. Our main interest concerns the width of the wall and the difference in the energy between  $\gg||\ll$  and  $\ll||\gg$  walls.

To describe a wall we must allow the tilt angle and smectic displacement to vary in the  $x$  and  $z$  dimension. Calculations in Section V.1 indicate that the layer slope is dominated by the strain imposed on smectic layers. Since in this case we are concerned mainly with phenomena related to the layer evolution we perform our study in the SmA phase (i.e.  $C_{\perp} > 0$  in Eq. (1)) and set  $\theta_t = 0$ . The strain imposed to smectic layers is induced by setting  $q_s/q_0 = 1.01$ . In calculations we allow the chevron tip reorientation via a quasibookshelf structure as reported in ref. /9/. Only a half of the wall is calculated since symmetric conditions are assumed. At the center of wall the bookshelf structure is set and the bulk chevron structure far (with respect to  $L$ ) from the wall.

The evolution of the displacement field  $u(z) = \langle u(x,z) \rangle$  averaged over the cell thickness from the wall center is depicted in Fig. 8. The layers recover the conventional chevron structure (i.e. the structure not influenced by the wall) over a distance comparable to  $L$ . The widths

of the  $\gg||\ll$  and  $\ll||\gg$  walls are almost the same. Nevertheless the free energy  $F_{\ll||\gg}$  of the  $\ll||\gg$  wall, calculated from Eq. (1), is much larger than  $F_{\gg||\ll}$  of the  $\gg||\ll$  one ( $F_{\ll||\gg}/F_{\gg||\ll} \approx 2.2$  for parameters given in Fig. 8). Thus from the energy point of view the walls are quite different suggesting different scenarios of the wall organisation. In most cases zig-zag wall appears with the direction of the wall close to that of the layer normal. This is achieved by local layer slip at the surface in such a way that strain imposed on smectic layers in the cell is relaxed to a great extent. Consequently the wall width  $\xi_d$  is substantially reduced /2/.

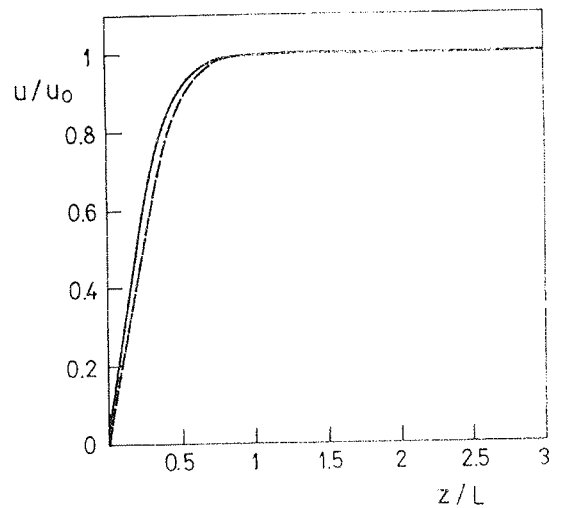


Fig. 8  $u(z) = \langle u(x,z) \rangle$  as a function of  $z$  for  $\ll||\gg$  and  $\gg||\ll$  head on head chevron tip transitions.  $\theta_t = 0$ ,  $q_s/q_0 = 1.01$  and the other parameters are the same as in Fig. 6. The  $\theta(z) = \langle \theta(x,z) \rangle$  dependence has similar dependence. For the parameters chosen the harmonic approximation /3,4/ works well, thus  $du(x,z)/dx \approx \tan(\theta(x,z))$ .  $u_0 = u(z > L)$ , the domain wall is at  $z = 0$ .

## VI. DISCUSSION OF EXPERIMENTAL DATA

In order to qualitatively explain the photographic picture shown in Fig. 5 we use the results of the model studied in the previous section. The variation of the slope of the surface in the  $z$ -direction in the experiment is modelled by spatially dependent pretilt angle  $\theta_t$ . As shown in Fig. 4 we divide the sample into regions (i),(ii),(iii),(iv) and (v). The pretilt  $\theta_t = \theta_p \approx 3^\circ$  in regions (i),(iii) and (v) is achieved by a nylon surface treatment. The left slope of the region (ii) is simulated by the surface tilt  $\theta_1 = \theta_s + \theta_p \approx 30^\circ$  and the right one of the region (iv) by  $\theta_r = -\theta_s + \theta_p \approx -23^\circ$ .

According to our findings the stability and existence of C1 and C2 structures strongly depend on the ratio  $\chi = \theta_c/\theta_t$ . The experiment was performed at the temperature corresponding to the bulk tilt angle  $\theta_c \approx 22^\circ$ . Thus in regions (i), (iii) and (iv) the ratio  $\chi \approx 0.14$  is well below the

critical value  $\chi_{C2} \approx \chi_{C1} \approx 1.7 \pm 0.4$  estimated for our model structures. In these regions the C2 structure has slightly lower free energy than C1. The situation is similar in the region (iv) where  $\chi \approx 1.1$  but in this case the energy difference between C1 and C2 is larger. In the region (ii) the ratio  $\chi \approx 1.4$  is within the regime where according to our estimates the transformation to the C1\* structure is expected.

To get an impression where zig-zag defects tend to form we neglect coupling between different regions. If the critical condition is not fulfilled in the region (ii), the C2 structure is locally enforced in the whole sample. But because of different tilt direction in region (iv) the sequence of tilt orientations according to the model system shown in Fig. 4b is  $>1>2>3<4>5$ , where, e.g.,  $>3$  describes the chevron kink to the right at the region (iii). If the critical condition is fulfilled in (iv) then the sequence is  $>1<2>3<4>5$ . Thus in the decoupling approximation in both cases zig-zag defects tends to be formed. In the following we show that if coupling is taken into account both cases are expected to give similar qualitative appearance.

We first note that broad straight walls characteristic for the head to head chevron collision are not expected for the following reasons. The width of the sloped region is far less than  $L$  what is required for the realisation of the head to head chevron collision. The corresponding correlation length  $\xi_d \approx L \approx 1.5 \mu\text{m}$  is much larger than the width  $\Delta H_z \approx 0.2 \mu\text{m}$  of the sloped regions. Thus at slopes, where the flip of the chevron tip is expected, only a zig-zag like wall is plausible which requires less space and the elastic free energy costs for its realisation. The experimental results confirm this expectations. Only walls with strong zig-zag appearance are observed as it is evident from Fig. 5.

We then assume that in the region (ii) the critical conditions are fulfilled and consequently predict the spatial evolution of the chevron tip orientation structure from the left to the right in Fig. 4. In the semiinfinite region (i) the C2 chevron profile with the kink to the right is realised. In (ii) the C1\* structure is enforced with the kink to the left leading to the zig-zag formation. Let us suppose that the first step triggers the zig-zag defect and try to figure out the chevron tip orientation in the region (iii) between the two sloped stripes. There free energies of C1 and C2 are comparable because of a low pretilt. Both slopes enforce the kink to the left (first via C1\* and second via the C2 structure which is at the second slope much more favourable with respect to C1 because of a relative large value of  $\theta_t$ ). Consequently the slightly metastable C1 structure with the kink to the left is most probable in between. Thus in the region (iii) only rarely additional zig-zag defects are expected because the driving force for it is small due to similar free energies of C2 and C1 structures. But the semiinfinite region (v) enforces the C2 structure with the right chevron kink orientation. Thus if the zig-zag defect was formed at the first step then the another zig-zag defect is expected at the second slope in accordance with experimental observation.

Note that the zig-zag defects appear at slopes because (i) they enforce the flip of the chevron tip and (ii) the AFM

photographs reveal that at the top the slopes are relatively rough serving as seeds for the zig-zag defects. Recent experiments [2,8] reveal that the zig-zag defects are most often pinned to the surface irregularities.

The experiment reveals that at the first slope the zig-zag lines are pushed more toward the straight region (i) while at the second slope the defect lines extend also over the sloped region. This is understandable because at the first slope only the C1\* structure is expected while at the second both C1 and C2 structures are allowed. Consequently at the first slope the zig-zag defect, triggered by the slope and seeds at its edge, is pushed towards the region (i). At the second slope the flip of the chevron tip realised via the C1 to C2 transformation is also allowed at the slope. Nevertheless it is advantageous for zig-zag defects to form at the straight region (iv) where the free energy difference between the structures with the opposite tip orientation is relatively small.

In the case that also  $\theta_1$  is below the critical value C2 tends to be established in all regions. But due to the sign variation in  $\theta_t$  the chevron tip tends to be aligned to the left in the region (iv) and to the right in all other regions. Thus also in this situation at least 2 zig-zag lines are expected in the  $z$  direction if they are initiated. The most probable site to trigger them is the second slope in which the energy difference between the C1 and C2 structure is the largest. The first zig-zag line is thus formed at the border between regions (v) and (iv). On entering the region (iii) another chevron tip orientation is enforced. But most probable it persists till the region (ii), where this tendency is larger because of larger effective tilt angle and the surface irregularities at the top of a slope that trigger the zig-zag formation.

Thus in both cases ( $\chi_1 > \chi_{C2}$  or  $\chi_1 < \chi_{C2}$ ) two zig-zag lines at the slopes are expected. Nevertheless in the second case the probability for this formation is lower because both structures can exist in the whole region.

## VII. CONCLUSIONS

In conventional LC cells filled with SmC LC the so called zig-zag defects are commonly observed. It is believed that surface imperfections are potential sources for their creation. To check this hypothesis we study experimentally and theoretically the influence of sloped surfaces on the chevron structure.

In the experimental part of the work we demonstrate that the sloped regions are strong sources of zig-zag defects. We formed a slope with rather well defined inclination and studied its influence on the chevron tip reorientation. The photographs obtained with polarised microscope reveal zig-zag loops almost exclusively formed at the sloped regions.

In order to explain qualitatively the photographs we study the influence of surface pretilt on C1 and C2 chevron structures in SmC LC. A phenomenological model is used. For simplicity we confined our interest to planar structures and strong positional and orientational anchoring. We introduce the ratio  $\chi = \theta_t / \theta_c$  between the pretilt angle  $\theta_t$  and the smectic tilt angle  $\theta_c$  which most significantly predicts the chevron tip orientation. A

threshold behaviour is observed as a function of  $\chi$ . Below a critical value of  $\chi$  both C1 and C2 structure exist but only C2 structure seems to be stable. Above threshold both structures convert into the identical structure, that we name the C1\* structure. The basic difference between C1 and C1\* structure is wider chevron tip in the latter case. For supramicron cells this distinction is hard to be experimentally observed. Then we limit our attention to the structure and free energy of the zig-zag wall which runs parallel to smectic layers. We show that the width of both  $\langle\langle||\rangle\rangle$  and  $\langle\rangle\rangle||\langle\rangle$  walls is comparable and roughly given by the cell width. The free energy of the former wall is considerably higher what forces the LC to find another realisation of the chevron tip reorientation. Most of the prediction steaming from our rather simple model are in accordance with recent experimental observations. Based on our estimates we qualitatively explained the observed zig-zag patterns. In the explanation we assumed that surface pretilt can to a good approximation imitate the influence of a sloped region.

In the theoretical part of this work we made several simplifying assumptions. Agreement between theoretical predictions and experimental observations supports the belief that the model exhibits at least qualitative most of the phenomena of interest. The study in which we relax most of the simplifying assumptions in order to get better quantitative estimates is currently under way.

### Acknowledgements

We gratefully acknowledge ass. prof. I. Muševič for making the AFM images of the polymer surfaces. The research was supported by Copernicus grant #CP940168 as well as Slovenian Ministry of Science and Technology (Grant No.J1-7067, J2-7609-0589-96) and TMR Research Network Proposal ERB4061PL970397.

### LITERATURE

- /1/ P.G. de Gennes and J. Prost, *The Physics of Liquid Crystals* (Oxford University Press, Oxford, 1993).
- /2/ N.A. Clark, T.P. Rieker, and J.E. MacLennan, *Ferroelectrics* 85, 79 (1988).
- /3/ L. Limat and J. Prost, *Liq.Cryst.* 13, 101 (1993).
- /4/ S. Kralj and T.J. Sluckin, *Phys.Rev.E.* 50, 2940 (1994).
- /5/ N. Vaupotič, S. Kralj, M. Čopič, and T.J. Sluckin, *Phys. Rev. E.* 54, 3783 (1996).
- /6/ M. Cagnon and G. Duran, *Phys.Rev.Lett.* 70, 2742 (1993).
- /7/ Y. Ouchi, Y. Takanishi, H. Takezoe, and A. Fukuda, *Jpn.J.Appl.Phys.* 28, 2547 (1989).
- /8/ J. Kanbe, H. Inoue, A. Mizutome, Y. Hanyou, K. Katagiri, and S. Yoshihara, *Ferroelectrics* 114, 3 (1991).
- /9/ A. Iida, T. Noma, and H. Miyata, *Jpn. J. Appl. Phys.* 35, 160 (1996).
- /10/ J. Pirš et al., to be published.
- /11/ J. Watson, P. Bos, and J. Pirš, *Phys.Rev.E* 56, R3769 (1997).
- /12/ J. Pirš, S. Kralj, S. Pirš, B. Marin, P. Watson, C. Hoke, and P. Bos, 16th International liquid crystal conference, Kent State University, Ohio (1996), Abstract book, P-170.

*J. Pirš, R. Petkovšek, S. Pirš,  
S. Kralj and S. Žumer  
J. Stefan Institute,  
Jamova 39, 1000 Ljubljana,  
Slovenia  
email: janez.pirs@ijs.si*

*Prispelo (Arrived): 22.4.1998*

*Sprejeto (Accepted): 29.4.1998*